High Speed Schlieren Imaging And PIV Of Unsteady Free Jet Injection With Plume Formation

Mario K. Peyha[1,*], and Christian Weiß[1]

1: Chair of Process Technology and Industrial Environmental Protection, Montanuniversität Leoben, Austria
* Correspondent author: mario.peyha@unileoben.ac.at

Keywords: seedingless, schlieren image correlation velocimetry, PIV-algorithm, unsteady gaseous jet injection, plume formation

ABSTRACT

The aim of this work is to investigate schlieren image correlation velocimetry for flow field quantification of gaseous jet injection in non-manipulable apparatus like flow chambers. Such flow cases often struggle using tracer-based methods: Seeding particles may locally cause technical problems, or the plant design prevents principal opportunity of tracer adding, both of which lead to a reduced method repertory. This is specifically the case under flow conditions, where contamination of apparatus internals by seeding particles should be avoided completely.
Therefore, in this paper we explore a seedingless, refraction-based method to quantify the velocity field of a jet plume. As experimental flow case we examine a transient jet release into a closed compartment under nearly atmospheric conditions. For simplification and greater clarity, the laboratory model geometry is kept essentially two-dimensional, thus we chose a flat-jet nozzle as injection device. The experimental investigations cover high speed schlieren imaging and laser sheet visualization followed by digital image correlation. Combining the traditionally qualitative schlieren approach for flow visualization with Fast Fourier Transform and cross-correlation algorithms, we calculated the velocity vector field of an unsteady jet plume formation. Furthermore, we determined the axial jet velocity profile at steady state conditions. Our research findings highlight the applicability of schlieren image correlation velocimetry to spatially quantify gaseous jet formation at encased flow sections. Concluding, the results coincide with data from particle image velocimetry measurements and point out the potential of expanding flow diagnostics to hitherto hardly explored (industrial) flow cases.

1. Introduction

For decades tracer-based optical methods have formed a state-of-the-art in flow diagnostics. However, seeding the flow volume is often cumbersome or impossible. The latter especially applies to industrial spray applications and gaseous nozzle flow. In this case inner flow geometry may introduce limitations by nozzle diameter or slit height. Our investigation concentrates on a gaseous jet injection with specific emphasis on the unsteady diagnostics of the jet onset and resulting plume formation. Hereby, potential particle clogging at any precisely manufactured

nozzle outlet or alternatively homogeneous, indirect seeding of the outer flow field might cause considerable experimental challenges.

Recently, a couple of emerging image acquisition and processing techniques, such as background-oriented schlieren (BOS) (Raffel, 2015; Settles & Liberzon, 2022) and schlieren image correlation velocimetry (SICV) (Biswas & Qiao, 2017; Settles, 2001), provide concepts to circumvent the seeding issues. Both of them utilize refractive index gradients for flow visualization. These occur in case of local density or concentration gradients within a fluid or, alternatively, when fluids of different refractive index get in contact. BOS undeniably attracts with its simple optical setup and, due to the present standard of computer power, for velocity field quantification. Though, investigating fine flow structures with BOS is challenging. Caused by two discretization steps necessary (firstly creating a pseudo-schlieren image and afterwards calculating the velocity field) the image resolution, hence vector quantity or density, might drop dramatically relative to the raw image. So, a 1000x1000 pixel raw image will result in a velocity field of 10x10 vectors, if an interrogation window size of 10x10 pixels without overlap is used twice along two consecutive cross-correlation steps. In contrast to that, SICV enables schlieren to already appear at the raw image (i.e. 1000x1000 pixel) and offers high resolution vector fields (i.e. 100x100 vectors) by the necessity of only one cross-correlation step. Exactly this advantage we identified as key criterion for resolving small flow features, typically occurring in jet flows. Being aware of the complex optical setup, we chose SICV as promising method for performing the jet injection quantification, and, as complementary method to evaluate the SICV results, PIV with pre-seeding the test chamber.

Up until now, direct experimental based comparisons of SICV and pre-seeded PIV are scarce within the open literature. In our contribution, we focus on the non-intrusive flow diagnostics of unsteady free jet injection and likewise steady-state jet velocity, explicitly using the methods SICV and PIV.

Firstly, using SICV, we investigate a schlieren setup for flow field acquisition that offers time-resolved imaging of the jet injection features. On our test rig we contact two gases with significantly different refractive indices and relative velocity. Thus, schlieren occur locally and visualize the flow situation at the gas-to-gas interface. Furthermore, the velocity field is reconstructed from the schlieren images via double frame cross-correlation algorithms.

Secondly, we investigate the homogeneous gas jet injection in the particle pre-seeded test chamber with PIV. To illustrate demonstrability of refraction-based flow field quantification we compare the resulting vector fields of SICV and PIV. As local transient jet flow features change by onset time and operating conditions, we perform experiments for the following three test cases.

Therefrom, two test cases are chosen to examine jet plume formation and we complete the picture with a steady-state jet investigation as third test case.

2. Experiment

For the laboratory experiments, we first built a test rig mainly consisting of the test chamber, valves and sensors as well as a programmable logic controller. Depending on the optical diagnostic method we afterwards assembled the optical setup and finally, performed the jet injection experiments. The same flow situations are experimentally investigated with both SICV and PIV, slightly differing in the chamber preparation procedure (chamber purge with helium or pre-seeding with smoke particles).

Test Rig

The test chamber consists of a prismatic 3D-printed frame made of polylactic acid (PLA) which is housed between parallel glass panel (float glass) for investigation with optical methods. At the inlet an aluminum flat nozzle with a gap height of 0.05mm (Super Air Knife 110003 from EXAIR LLC.) is positioned. The outlet is part of the frame-glass-construction. Fig. 1 illustrates the test chamber, the area of interest for high-speed imaging (rectangle) and the flow to target.

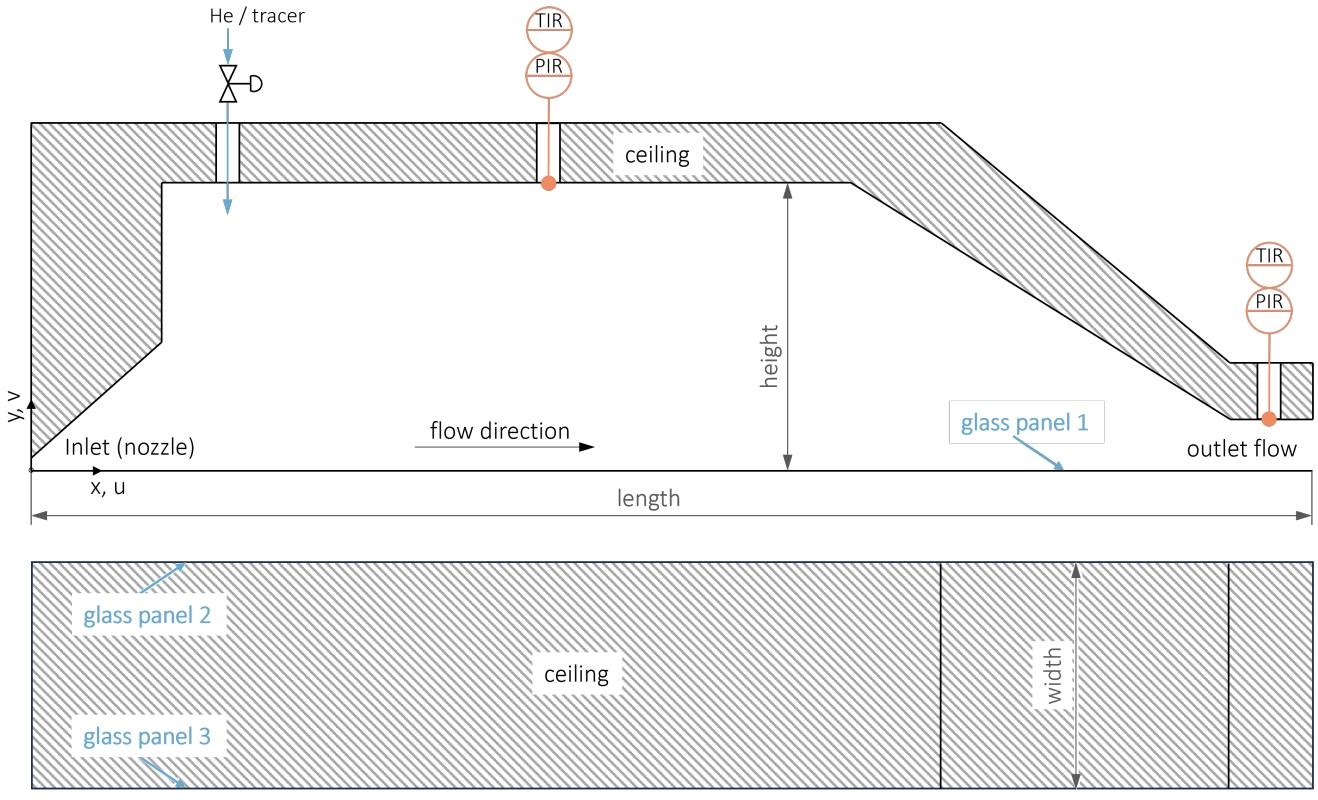

Fig. 1 Unsteady jet injection into the test chamber geometry (length = 600mm, height = 100mm, width = 80mm) with controlled helium or alternatively seeded gas inflow and continuous pressure and temperature monitoring.

Three solenoid valves (not detailed in Fig. 1) are mounted to the test chamber: the inlet valve upstream the nozzle (air inflow), the outlet valve (outflow), and the so-called purge valve (for adding helium or particles), that is mounted on the PLA-frame and situated perpendicular to the main flow direction. A compact controller (Siemens LOGO!) switches the valves on or off according to the developed purge or jet flow program, provides data acquisition and furthermore triggers the high-speed camera. Downstream the outlet valve a ventilator transports the gas and particles to the exhaust air system and additionally offers negative outlet pressure during the chamber purge program. The characteristic opening time of the valves is in the order of 17 +/- 3 milliseconds and was investigated to be pressure independent in the experimental range of 1 to 6 bar pipe pressure.

Flow Situation

The unsteady free jet injection into the chamber is in the focus of the experimental investigation. Hereby, we pay specific attention to the emerging jet plume velocity field. For further quantification, the jet is studied at steady state. The three flow cases studied are specified in Table 1. The measured ambient pressure and temperature during the experimental investigation were measured with 947 +/- 2 mbar, and 24 +/- 2 °C, respectively. Whilst jet injection the chamber gauge pressure typically rose to 3mbar (Case 1) or 8mbar (Case 2 and Case 3), whereas the temperature response was marginal.

Table 1 Test cases for optical investigation of jet injection.

	Flow feature	Condition	Time from onset	pipe pressure
Case 1	Jet plume	Unsteady state	8.6 ms	1 bar
Case 2	Jet plume	Unsteady state	8.6 ms	3 bar
Case 3	Formed Jet	Steady state	600…700 ms	3 bar

Optical Setup

The high-speed schlieren imaging experiments were performed using a z-type schlieren setup (Schardin, 1942; Settles, 2001, p. 42), extended with two plane first-surface folding mirrors, as shown in Fig. 2. The main parts consist of a high-speed LED lamp (Veritas Constellation 120) as pulsed light source (pulse time: 5 μs, frequency: 10kHz), a planoconvex lens, an adjustable optical slit (width: 1mm, height: 6.2mm) two identical parabolic mirrors (diameter: 150mm, focal length:

1.22m), two plane mirrors (diameter: 38mm), a razor blade and an ultra-high-speed camera (Phantom v2512, recording rate: 10,000 fps, exposure time: 3μs). The vertical cut-off (both slit and razor blade vertically aligned) was set to approximately 80%. By contacting helium and air local density gradients form, caused by the with highly different refractive index n of the two gases; $n_{He,0°C} = 1.000036$ and $n_{Air,0°C} = 1.000293$ at $\lambda = 589.29$nm (Hecht, 2017). Hence, refractive index gradients are present and, consequently, schlieren (S) appear.

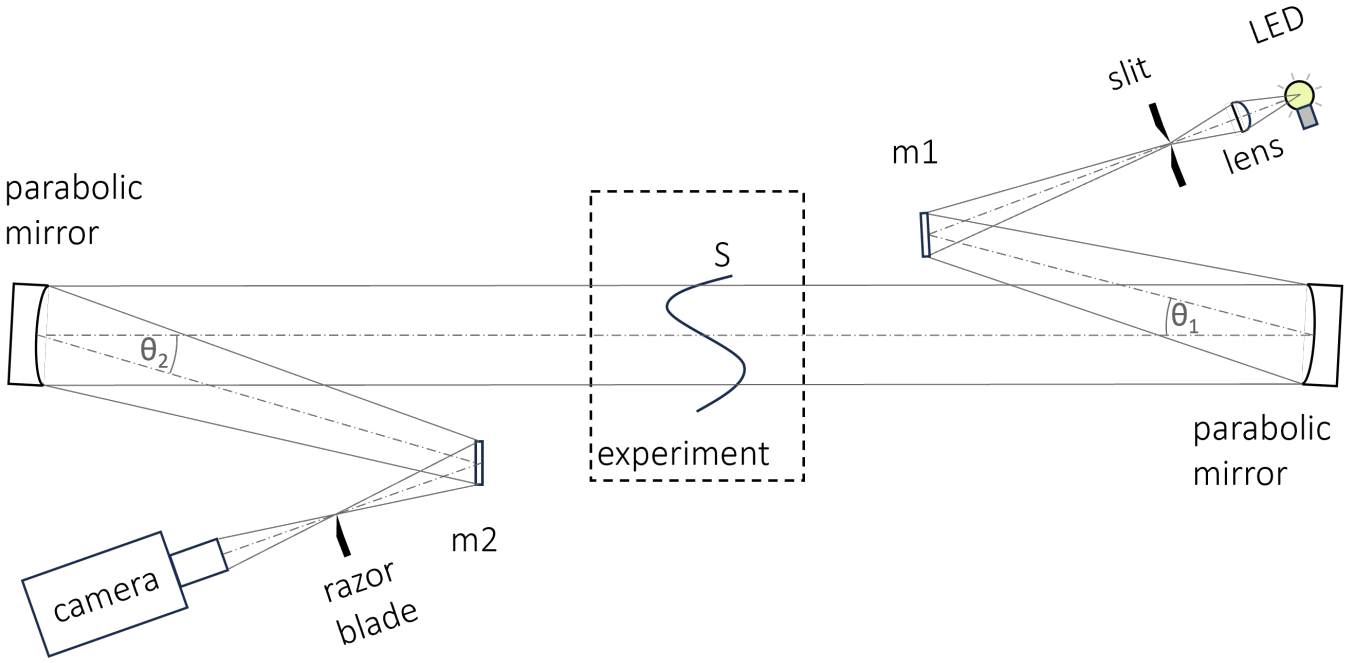

Fig. 2 Z-type schlieren setup with plane first-surface folding mirrors (m1, m2) with $\Theta_1 = 6.5°$ and $\Theta_2 = 5.0°$

For the PIV experiments the setup follows a standard light sheet imaging configuration, with an inclination towards the vertical axis of the laser beam to ensure the lighting of the nozzle outlet, as shown in Fig. 3. A dual head diode pumped Nd:YLF laser (Litron LDY303HE PIV) realized double frame lighting (pulse duration: 150ns, pulse energy: 2.5mJ) and recording at a frame rate of 10kHz. The interframe time and the time between to laser pulses were set to 25μs.

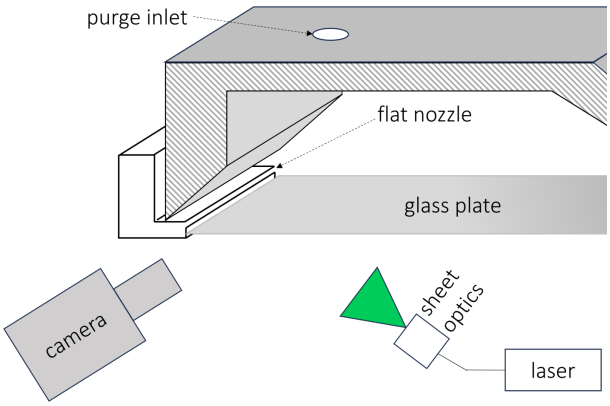

Fig. 3 PIV-Setup with inclined sheet optics and chamber pre-seeding through purge inlet

Experimental Procedure

Firstly, the chamber is flooded with helium (for schlieren imaging and velocimetry) or alternatively pre-seeded with smoke particles (for PIV) using the purge valve, outlet valve and fan (purge program).

After purging and a settling time of approximately 7 seconds the jet flow program launches: The inlet and outlet valve open and an air jet is flowing through the nozzle into the chamber. At the same time both the pulsed illumination and the high-speed recording start and last for 2 seconds. The captured images are saved and subsequently processed. For both image recording and processing the software DaVis, version 8.40 (LaVision GmbH) was used.

3. Quantification

The main steps for the development of the raw images to the reconstructed schlieren velocity field cover scaling, image preprocessing and double frame cross-correlation.

Scaling

Here, scaling estimates the relationship between the real physical dimensions and the camera sensor pixel size. For this purpose, calibration plates are considered as standard reference. As we focus on flow situations where the gas volume during the experiment remains inaccessible by mechanical means, we rely on in-focus objects with known dimensions. In our case, the chamber height (parallel top and bottom edge) was used as reference length. Thus, the coordinate system was scaled and checked at different image positions of known object size.

Image Preprocessing

The raw image is processed according to the following steps (in chronological order):

1. Image mapping and enhancement (mirroring, rotating, contrast stretching)
2. Background subtraction (subtraction of time-averaged images before jet injection occurs)
3. Linear filtering 1 (Gauss smoothing and diagonal Sobel filter, both for 3x3 pixel areas)
4. Linear filtering 2 (sharpening, medium, 3x3 pixel areas)
5. Image reorganization (conversion of consecutive time-series single-frames to double-frames); obligatory for double-frame cross-correlation

The preprocessed image allows a tracking of local flow features, i.e. eddy substructures. Fig. 4 shows the mirrored raw schlieren image and the preprocessed image

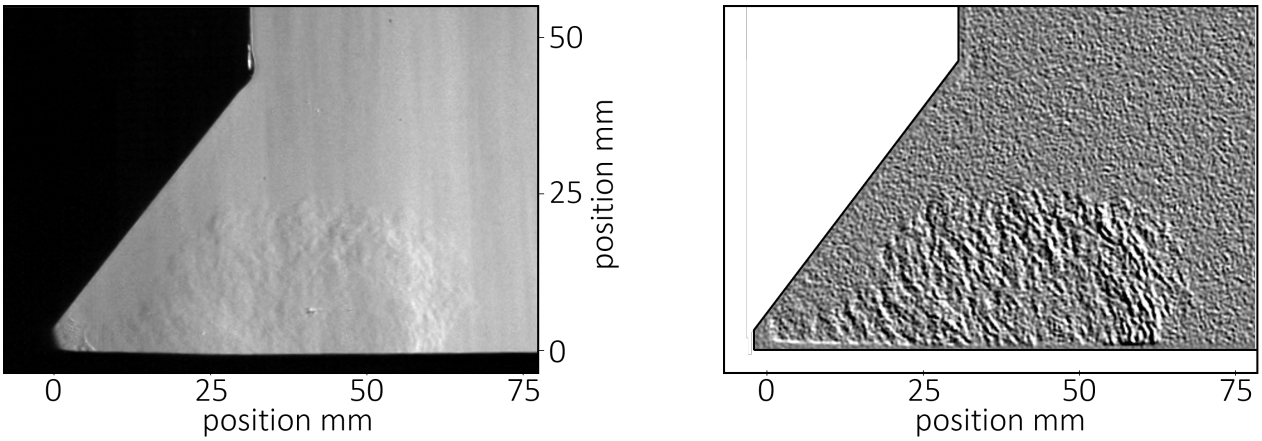

Fig. 4 Schlieren recording of jet injection. Mirrored raw image (left) and preprocessed image (right) for calculation.

Velocity Calculation

After image preprocessing, the double-frames (or image pairs) are processed using an FFT-based cross-correlation algorithm – usually used for PIV – with multiple passes and decreasing interrogation window size (64x64 px -> 32x32 px, elliptical shape rx = 2ry, 75% overlap, 2 initial and final passes). The local flow feature displacement combined with the camera recording rate leads to a two-dimensional velocity vector in each interrogation window. Analogously, correlating consecutive single-frames of a time-series (by dropping preprocessing step 5) might produce identical results.

Spurious vectors and artifacts are reduced by vector post-processing. In detail, a median filter for universal outlier detection, a vector magnitude filter, spatial smoothing filter (area for all steps: 3x3 pixels) were used and vector groups of < 3 vectors were removed.

Fig. 1b and 1c illustrate the raw schlieren image and reconstructed velocity field at the reference jet injection time of 8.6ms, where the jet plume filled approximately 80 per cent (50 mm) of the total frame length imaged.

The laser sheet images for PIV were preprocessed as well. Hence, we applied image mapping (mirroring), background subtraction and, moreover, intensity normalization to ensure homogeneous light intensity and further enhance particle image quality.

The velocity calculation parameters for the PIV measurements were set the same as for the schlieren image quantification, initially using double frames with an interframe time of 25μs instead. What is more, a significantly lower number of spurious vectors was observed than with

SICV. However, to keep comparability of both methods, the same post-processing features were applied. Fig. 5 shows the raw images of schlieren and laser sheet recording. The visualization of the resulting velocity vector fields is illustrated and discussed in section 4.

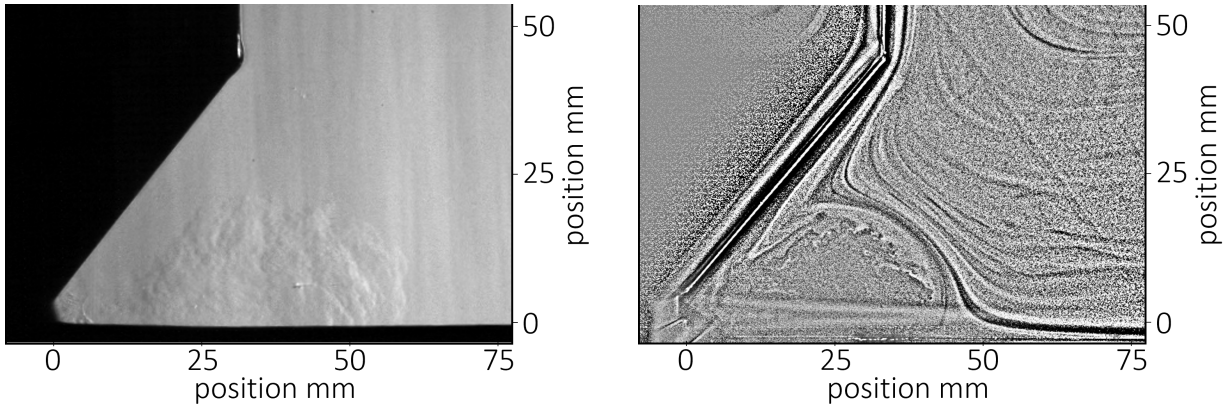

Fig. 5 Mirrored raw schlieren image (left) compared with intensity normalized particle image (right) for Case 1.

4. Results and Discussion

Experimental investigations with SICV and PIV were performed for Case 1, Case 2 and Case 3, as listed in table 1. With a time resolution of 0.1 milliseconds, a synchronization and further direct comparison of schlieren- and laser-based high speed images and velocity fields were realized. Firstly, the unsteady jet injection was analyzed for Case 1 and Case 2. Fig. 6 illustrates the comparison of the velocity fields calculated with SICV (left) and PIV (right). Note, that choosing different camera image resolutions cause a finer mesh at the PIV velocity vector field. The horizontal jet head position at Case 2 is further downstream than that at Case 1. As in both cases the same time stamp was chosen with $t = 8.6$ms ($t = 0$ms for jet head initially appearing at $x = 0$mm), the jet head penetration must be faster at Case 2, doubtlessly caused by the higher injection pressure. Comparing SICV with PIV, we observe a similar shape of the jet head in Case 1 and Case 2. Furthermore, the velocity values are of the same order of magnitude. However, the jet head position for each case does not match perfectly. The latter might be a result of the different optical setups, where only for SICV perfect parallel light rays cross the experiment. Consequently, slight perspective distortion at PIV might cause a horizontal shift of the initial jet head tracking position.

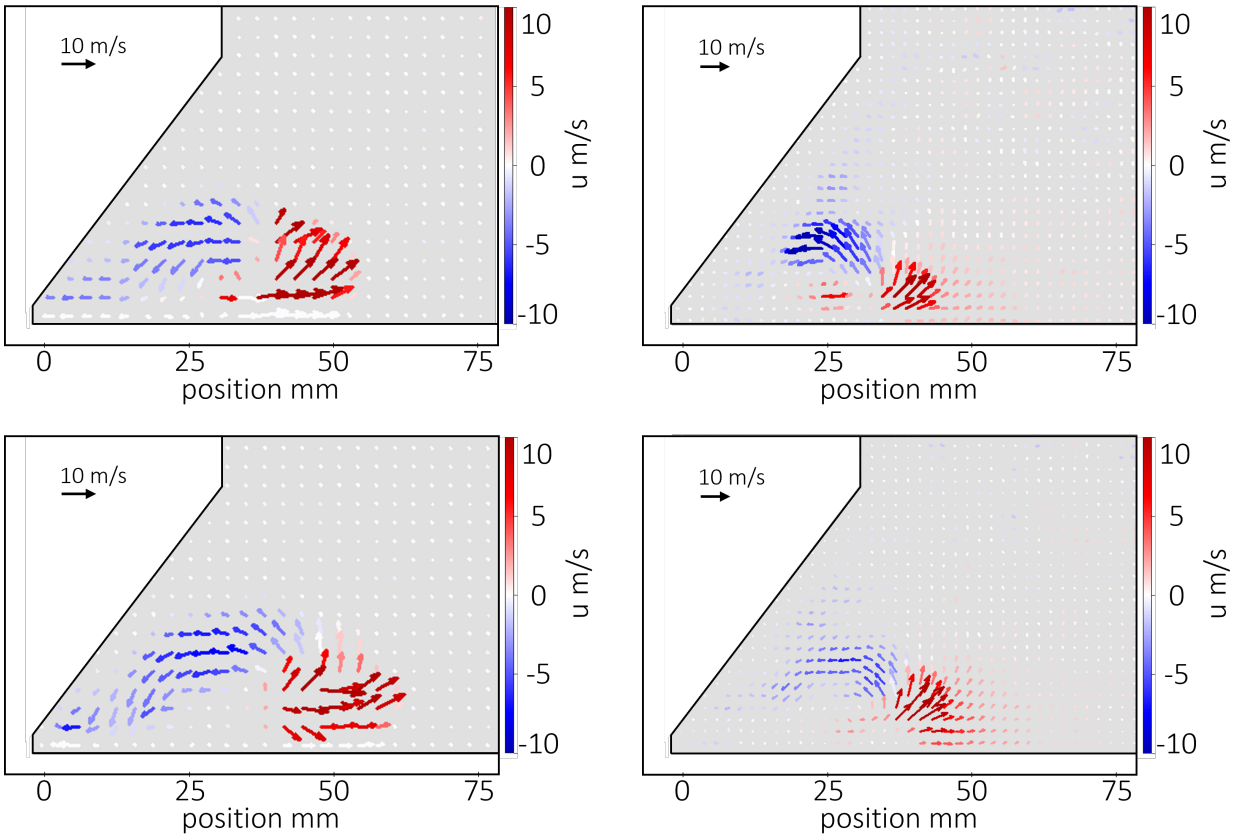

Fig. 6 Velocity vector fields of the jet plume for Case 1 (top) and Case 2 (bottom) at t = 8.6ms after jet onset, calculated with SICV (left) and PIV (right).

Furthermore, the flow field for Case 3, at steady-state, was examined and the time-average of 200 consecutive vector fields was calculated. Fig. 7 (a) shows the comparison of the time-averaged velocity profiles determined with SICV (helium jet in air) and PIV. The velocity profile was measured at a distance to the nozzle outlet of x = 70mm, which equals 1400 times the nozzle height. Apart from slightly differing values, the SICV velocity profile agrees in principle (shape and order of magnitude) with that of PIV. Focusing on the maximum velocity, SICV underestimates the absolute values at the streamwise as well as at the anti-streamwise direction with approximately 30% and 10%, respectively. To also gain time-depending information, the root-mean-square (RMS) velocity field was determined. At the position of maximum velocity, the ratio of the axial RMS velocity to maximum velocity was estimated with $u_{RMS,SICV} / \bar{u}_{max,SICV} \approx 0.13$ $(y/h = 0.014)$ and $u_{RMS,PIV} / \bar{u}_{max,PIV} \approx 0.43$ $(y/h = 0.027)$, respectively. Moreover, the spatial resolution close to the wall $(y/h < 0.01)$ was observed to be higher for PIV than for SICV, as shown in Fig. 7 (b).

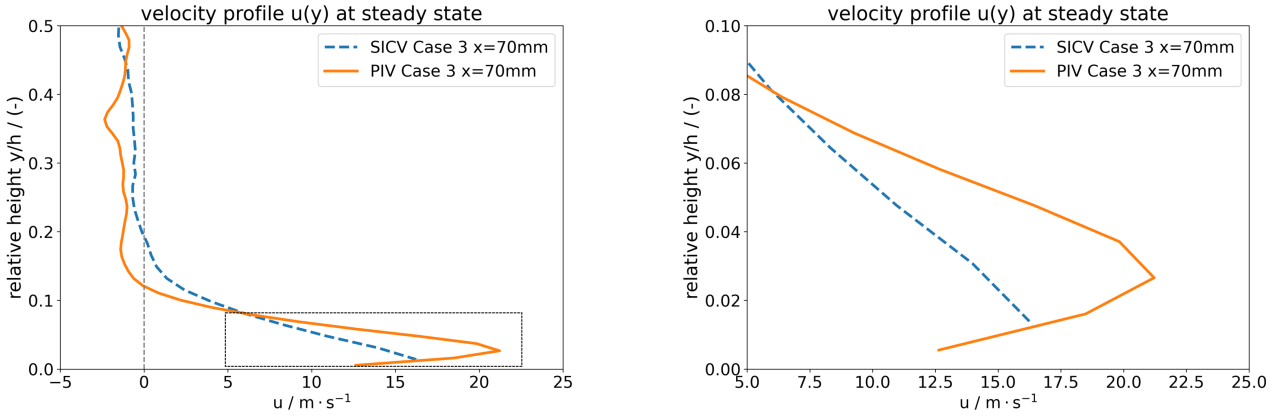

(a) (b)

Fig. 7 Streamwise velocity profile u(y) of Case 3 at a distance to the nozzle outlet of x = 70mm, measured with SICV (helium jet in air) and PIV for $y/h < 0.5$ (a) and the marked section magnified (b).

Fig. 8 (a) illustrates the raw schlieren image for Case 3, where the wall jet has already formed. Fig. 8 (b) and Fig. 8 (c) show the related vector fields. Here, the velocity fields of SICV and PIV show similar wall jet width at approximately x > 50mm. Although further upstream the lateral shear layer is hardly resolvable within PIV, we find distinct features of the wall jet profile within SICV. Furthermore, we can observe the jet (head) development and locate the boundary layer's growth, especially by comparing the raw images with their related vector fields.

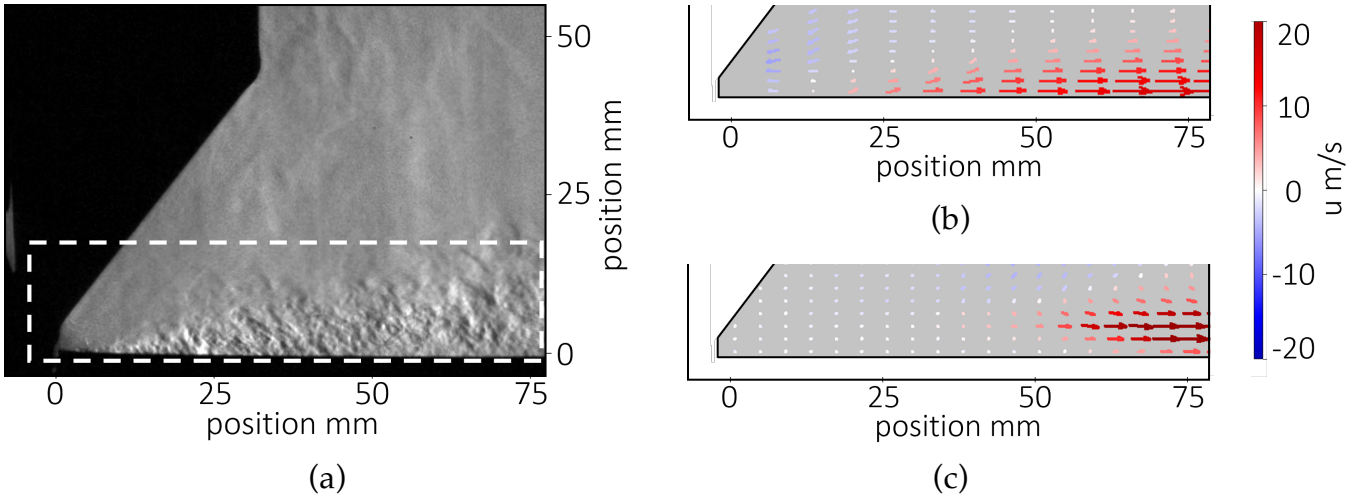

Fig. 8 Steady-state jet injection of Case 3. The marked section at the schlieren image (a) shows the target area for the calculation of the velocity vector fields with SICV (b) and PIV (c).

5. Conclusions

In this study, we investigated the jet injection process in a laboratory scaled test chamber with a high-speed schlieren imaging setup. Specifically, the prismatic test chamber was purged with helium before air was injected through a flat nozzle. Schlieren, that appear locally at shear or boundary layers of the two contacted gases (of different refractive index) offer semi-quantitative results like spatial- and time-resolved jet plume development, and moreover, with image processing and correlation methods, flow field quantification. In this manner, seedingless two-dimensional velocity measurements of unsteady and steady jet injection using SICV were successfully performed for three flow cases. Explicitly, elaborated image (pre)processing results were obtained by identification of trackable flow features with double frame FFT-based cross-correlation.

As a complementary measure, PIV data from a particle pre-seeded variant of the experiment are compared with SICV. Hereby, for unsteady jet injection, we observe nearly identical jet plume shape and eddy velocity fields of the same order of magnitude. To highlight the opportunity of jet velocity estimation at steady state, the ratio of the absolute maximum velocity $u_{max,PIV}/u_{max,SICV}$ equals 1.3 for streamwise and 1.1 for anti-streamwise direction, respectively. However, a general statement regarding uncertainty or measurement error would need further investigations. In general, using a vertical cutoff and parallel directed light rays crossing the field of observation, SICV offers the advantage to maintain the boundaries of the investigated flow domain always concisely defined. Additionally, even close to the wall a high spatial resolution of the vector field is supported.

Summarized, the results show the potential of the SICV method for process investigation where particle seeding and plant section manipulation are troublesome. Hence, the SICV method widens the field of velocity field measurement to applications with only one-axis optical access (no perpendicular laser or light sheet possible or necessary).

Aiming for high spatial resolution results, we mainly benefit from the advantages of the non-invasive schlieren setup for investigating flow phenomena with very short characteristic time constants and slow to moderate flow regimes, which in our setup was restricted to $Ma < 0.1$.

References

Biswas, S., & Qiao, L. (2017). A comprehensive statistical investigation of schlieren image velocimetry (SIV) using high-velocity helium jet. Experiments in Fluids, 58(3). https://doi.org/10.1007/s00348-017-2305-2

Hecht, E. (2017). *Optics* (Fifth edition, global edition). Harlow, Essex: Pearson.

Raffel, M. (2015). Background-oriented schlieren (BOS) techniques. Experiments in Fluids, 56(3). https://doi.org/10.1007/s00348-015-1927-5

Schardin, H. (1942). *Die Schlierenverfahren und ihre Anwendungen: Ergebnisse der exakten Naturwissenschaften*. Berlin.

Settles, G. S. (2001). *Schlieren and shadowgraph techniques: Visualizing phenomena in transparent media.* Engineering online library. Berlin, Heidelberg: Springer.

Settles, G. S., & Liberzon, A. (2022). Schlieren and BOS velocimetry of a round turbulent helium jet in air. Optics and Lasers in Engineering, 156, 107104. https://doi.org/10.1016/j.optlaseng.2022.107104